Eleventh U.S. National Conference on Earthquake Engineering
Integrating Science, Engineering & Policy
June 25-29, 2018
Los Angeles, California

PARAMETRIC STUDY ON DYNAMIC BEHAVIOR OF RC INTEGRAL BRIDGE INCORPORATING SIMPLIFIED SSI

S. Dhar[1] and K. Dasgupta[2]

ABSTRACT

The present study aims to investigate the influence of the length of an Reinforced Concrete (RC) Integral Bridge (IB) and the stiffness of foundation soil on its seismic behaviour. Two different types of foundation soil are considered, namely (a) medium stiff clay and (b) loose sand. To carry out Time History Analysis (THA), seven site specific ground motions are chosen from the site specific displacement spectrum in the program REXEL-Disp tool. From the THA, it is concluded that with increasing length of the IB, the deck-abutment-backfill integral system is subjected to higher seismic forces, making the abutment-foundation system more vulnerable to failure. Changes of foundation soil from loose sand to medium stiff clay can change the overall force distribution on piers and foundation piles. In loose foundation soil, bridge foundation is more flexible to deform and the structure is less susceptible to form plastic hinges during earthquake shaking. This feature is considered to be favourable for construction of larger jointless bridges.

[1]PhD Student, Dept. of Civil Engineering, Indian Institute of Technology, Guwahati, IN 781039 (email: sreya.dhar@gmail.com)
[2]Assistant Professor, Dept. of Civil Engineering, Indian Institute of Technology, Guwahati, IN 781039

Parametric Study on Dynamic Behavior of RC Integral Bridge Incorporating Simplified SSI

S. Dhar[1] and K. Dasgupta[2]

ABSTRACT

The present study aims to investigate the influence of the length of an Reinforced Concrete (RC) Integral Bridge (IB) and the stiffness of foundation soil on its seismic behaviour. Two different types of foundation soil are considered, namely (a) medium stiff clay and (b) loose sand. To carry out Time History Analysis (THA), seven site specific ground motions are chosen from the site specific displacement spectrum in the program REXEL-Disp tool. From the THA, it is concluded that with increasing length of the IB, the deck-abutment-backfill integral system is subjected to higher seismic forces, making the abutment-foundation system more vulnerable to failure. Changes of foundation soil from loose sand to medium stiff clay can change the overall force distribution on piers and foundation piles. In loose foundation soil, bridge foundation is more flexible to deform and the structure is less susceptible to form plastic hinges during earthquake shaking. This feature is considered to be favourable for construction of larger jointless bridges.

Introduction

Integral Bridges (IBs) have gained popularity over last few decades due to its easy to construct features and low maintenance cost as compared to the conventional bridges [1]. In an IB superstructure, abutments and backfill soil behave like a single unit, thus, special attention on forces and moments is required to accommodate extra movements and rotation of integral abutment system during earthquake shaking or thermal loading [2]. From several parameters (e.g., skewness of bridge, type of foundation type, type of backfill soil and type of foundation soil) which influence the overall behaviour of jointless bridge, the 'length' of an IB is expected to play an important role in the overall dynamic response. Thus, the present study is focused on the study of influence of the length of an IB on the overall seismic structural behaviour of the bridge. The effect of thermal variation on the bridge is neglected and considered as out of scope of this paper. In order to achieve the objective, a 3D bridge model, "inspired" by Humboldt Bay Middle Channel (HBMC) Bridge in California, is created using SAP2000 V.18 program [3] by eliminating any bearings or energy dissipating devices. Two types of foundation soil are considered, namely (i) medium stiff clay and (b) loose sand, to incorporate nonlinear dynamic soil-structure interaction at pile foundation and abutment backwall. In loose foundation soil, the foundation becomes more flexible which results in forming hinges at different locations of piles. IB with foundation in medium stiff clay has more chances of failure in pile foundation and pier columns.

[1]PhD Student, Dept. of Civil Engineering, Indian Institute of Technology, Guwahati, IN 781039 (email: sreya.dhar@gmail.com)

[2]Assistant Professor, Dept. of Civil Engineering, Indian Institute of Technology, Guwahati, IN 781039

Modelling

Structure and Foundation Properties

The geometry of the bridge is taken from Elgamal *et al*. [4] and the 3D model of bridge in SAP2000 is shown in Fig. 1. The original bridge consists of nine spans with the total length of 330m. Piers, piles, deck girders and cap beams are modelled as beam-column elements. Abutment walls, pile caps and deck slab are modelled as thin shell elements. Deck slab is supported on four I-shaped prestressed concrete girders. Deck and girders are rigidly connected with piers by cap beam. Abutments are 10m, 1.2m and 5m in breadth, width and height, respectively and are connected with foundation through 12m×3m sized and 0.7m thick pile cap. Piers are supported on 7m×7m×1m pile caps. Abutments and piers are supported on pile group foundation. Abutment foundation consists of 0.6m diameter reinforced concrete piles in double rows (9 nos.) and the pier foundation has a group of five precast driven RC piles each of diameter 1.372m. Abutment and pier piles are designed for axial compressions 500kN and 400kN, respectively.

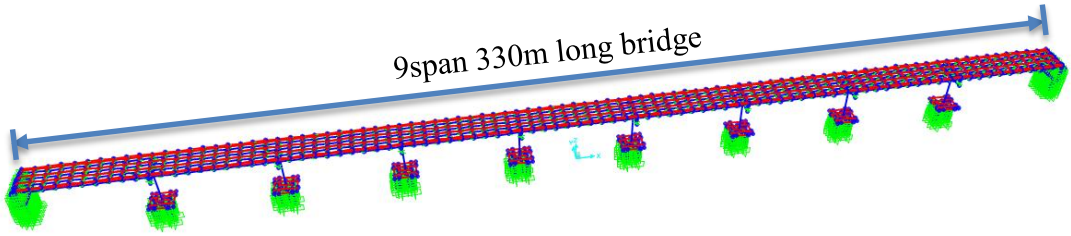

Figure 1. 3D bridge model in SAP2000 founded on medium stiff clay

Equivalent piers are modelled [4] keeping percentage of longitudinal reinforcement as 1% of gross cross-sectional area. Piers and piles nonlinearities are modelled using distributed fiber hinges. Pier and pile members are discretized into 3×3 fibers at cross section and 5-2 integration points along the length. The reinforcement details of the cross-section, with HYSD 415 bars, are shown in Fig. 2. The nonlinear material properties for core and cover concrete are considered using Chang and Mander's [5] model. Foundation embedded in medium stiff clay and loose sand are modelled with different lengths of piles depending on soil-pile load bearing capacity [6]. In medium clay, piles are 5.2m in length and in loose sand, abutment and intermediate piles are 10m and 15m in length, respectively.

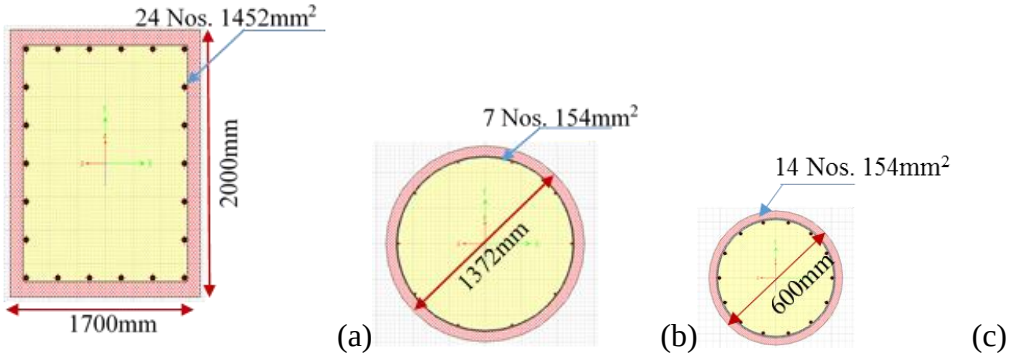

Figure 2. Reinforcement detailing of cross-sections for (a) pier, (b) pier piles and (c) abutment piles

Properties of Soil links

The considered properties of medium stiff clay and loose sand are given in Table 1. Nonlinear links are assigned at different locations of the pile foundation and abutment backwall (Figs. 3(a) and 3(b)). Links are modelled to take care of lateral bearing capacity (*p-y*), pile shaft skin friction (*f-y*) and pile tip load bearing capacity (*t-z*). Nonlinear links are modelled using 2-noded multilinear plastic force-deformation curves. Soil-pile interaction (SPI) is calculated from API [7] guidelines for medium clay and loose sand. For lateral Abutment-Backfill Interaction (ABI) (*f-y*) nonlinear curves to represent backfill soil are calculated from BA 42/96 [8] provisions. At the end of link's fixed end, input motions are applied as displacement time histories (DTHs). Those motions are extracted from the corresponding depth of the free field soil column under dynamic site response analysis. Thus, free-field GMs for the two considered soil cases are not the same. Abutment backwall links are modelled to take care of active and passive pressures of backfill soil.

Table 1. Soil properties used in the present study

Soil Type	Maximum shear modulus (MPa)	Poisson's ratio	Total unit weight (t/m^3)	Cohesion (kPa)	Internal friction angle
Medium stiff clay[1]	76	0.45	1.9	30	-
Loose sand[2]	55	0.45	1.6	-	29°

[1]after [9]
[2]after [10]

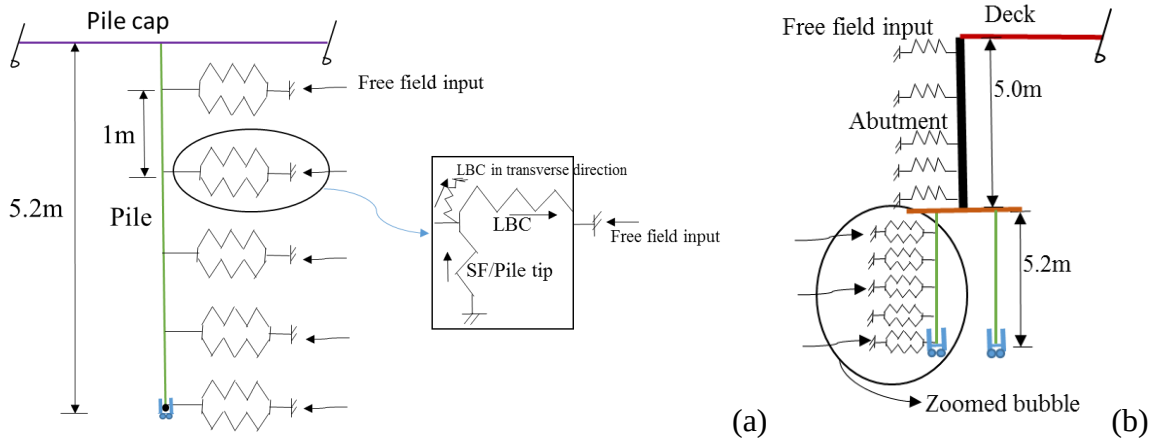

Figure 3. (a) Soil-pile interaction and (b) abutment-backfill interaction in medium stiff clay

Selection of Ground Motions

A bedrock Uniform Hazard Response Spectrum (UHRS) is used to select input Ground Motions (GM) for the analyses as discussed in Dhar *et al.* [11]. The UHRS is developed from the United States Geological Survey [12] national seismic hazard maps for the Humboldt Bay area for rock outcrop assuming the shear wave velocity, $V_{S,\,30m}$ as 800m/s (according to NEHRP [13], site

class B). The corresponding 5% damped elastic displacement response spectrum is given as the target specrum in the program REXEL-Disp [14] to select the ground motions for dynamic analysis from strong ground motion database SIMBAD [15]. The input parameters in REXEL-Disp to find the ground motions are: magnitude = 5.5-7.5; fault to site distance = 0-30km; spectrum matching tolerance = ±20%; spectrum matching period = 0.2s-5s; site specification = EC8 site class A, and the probability of exceedance = 10% in 50 years, representing a return period of 475 years. If a minimum of seven time histories are used for each component of motion, the design actions can be taken as the mean response calculated for each principal direction [16]. So, seven real record ground motions are chosen for application in the horizontal direction by scaling the response spectrum around the period of interest, such that the mean spectral response lies between the tolerances. The corresponding 5% damped elastic displacement spectra with the average of the ground motions are plotted in Fig. 4(a). For showing the results in the next section, two ground motions are selected for analysis, namely (i) GM#1 with PGA of 3.46m/s^2 and (ii) GM#2 with PGA of 0.725m/s^2.

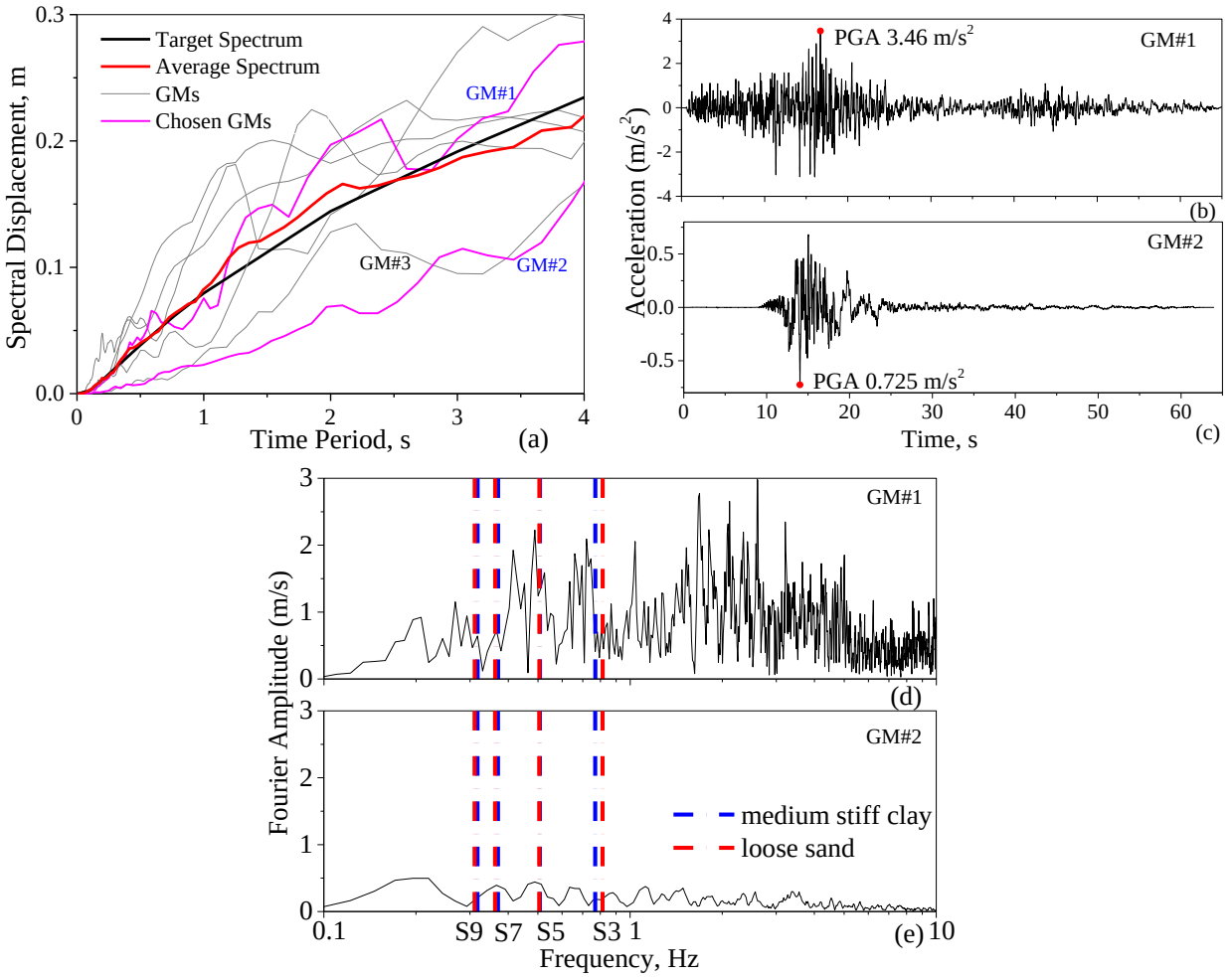

Figure 4. (a) Displacement spectra for all the GMs, (b) acceleration time history of GM#1, (c) acceleration time history of GM#2 chosen for parametric study, (d) Fourier amplitude of GM#1 and (e) Fourier amplitude of GM#2 [notations S9, S7, S5, S3 stand for 9span, 7span, 5span and 3span bridges natural frequencies].

Analysis

To investigate the effect of length, both end spans of the 9 span 330m length of IB are removed so that the bridge becomes a 7 span bridge of 257m length. Further successive removals of end spans transform the bridge into a 5 span bridge of 184m length and a 3span bridge of 112m length. End spans of the bridge are removed to reduce the overall length of bridge. Table 2. shows the natural periods of the different span bridges considered in the study. The natural periods of bridge models are in wide frequency range of 0.31Hz-0.81Hz. Bridge becomes more stiff with decreasing bridge spans. Figs. 4(b) and 4(c) represent the Acceleration Time Histories (ATH) of the chosen GMs. In Figs. 4(d) and 4(e), the Fourier transforms of ATHs of GM#1 and GM#2 are plotted and natural frequencies are marked for different bridge models considered in study. For GM#1, seismic energy input is higher beyond 1Hz of frequency, though there are few major peaks below 1Hz. For GM#2, seismic energy is distributed in broadband frequency range and Fourier amplitude is significantly lower than GM#1. In the first part of the paper, time history analysis is carried out on bridge models and nonlinear behaviour is investigated for medium stiff clayey soil with the variation of length and intensity of GMs. In the second part of the study, similar parameters are examined for the foundation in loose sand.

Table 2. Natural period of different span bridges considered in study

Soil type	9Span	7span	5span	3span
Medium stiff clay	3.15	2.70	1.97	1.30
Loose sand	3.22	2.76	1.98	1.23

Results

Response of bridge-foundation model in medium stiff clay soil

In medium stiff clay foundation soil, the 9span bridge under GM#1 yielded at piers (at 3rd and 6th piers' top), pier piles and abutment piles. The 7span and 5span bridges yielded at pier piles and 3span bridge remains linear elastic. Under GM#2, all the bridge models remain linear elastic. In the case of jointless bridge, forces on structure increase with increasing length of bridge. Figs. 5(a) and 5(b) show the Shear Force Time History (SFTH) at the top of the 3rd pier under GM#1 and GM#2, respectively. Under GM#1, due to higher intensity of PGA (i.e., 3.46m/s^2), Shear Force (SF) has significant variation among 9span, 7span and 5span bridges after t = 12.06s. Observing the nonlinearity, the residual SF is also highest for 9span bridge. In Fig. 5(c), the moment-rotation response at the top of 3rd pier shows that the pier has yielded and has become nonlinear after dynamic analysis. Under GM#2, i.e., at low intensity of PGA (i.e. 0.725m/s^2), SFTH of pier shows insignificant residual response in Fig. 5(b) and pier is linear elastic after dynamic analysis, which is evident from the moment-rotation curve shown in Fig. 5(d).

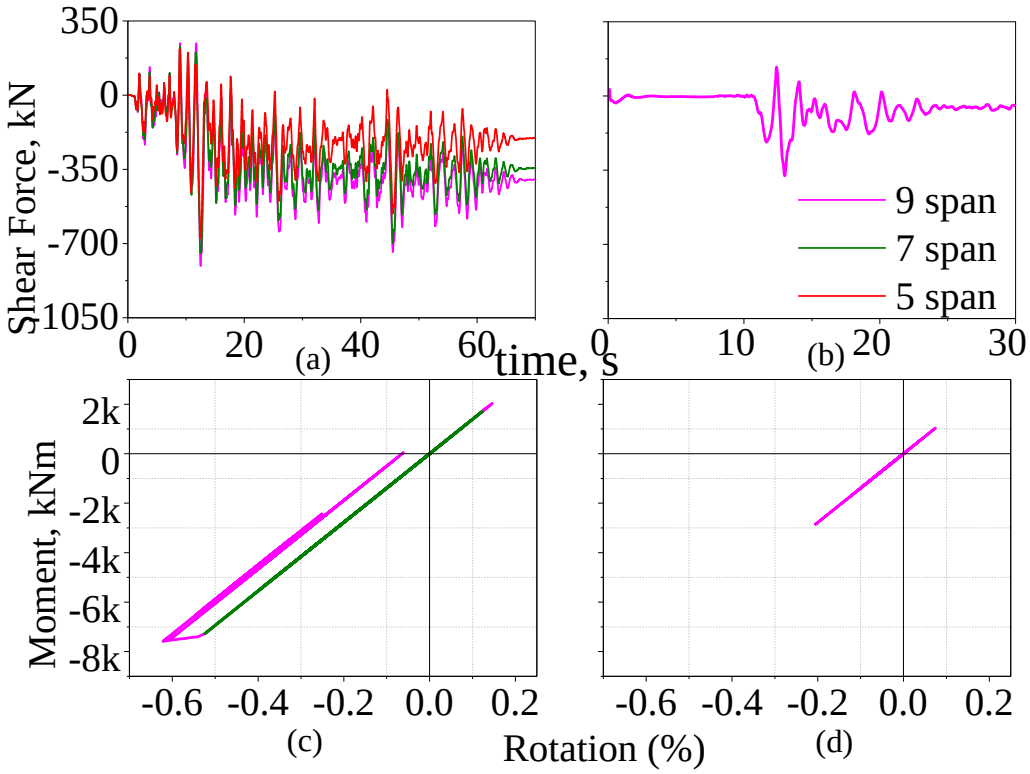

Figure 5. Shear force time history at the top of 3rd pier under (a) GM#1 and (b) GM#2; moment-rotation at the top of 3rd pier under (c) GM#1 and (d) GM#2 in medium clay soil.

Displacement Time Histories (DTHs) at the top and bottom of the abutments are monitored under GM#1 in Figs. 6(a) and 6(b), respectively. At the top of the abutment, 9span, 7span and 5span bridges have residual displacements of 24cm, 20cm and 14cm, respectively; this signifies that the 9span bridge has undergone highest extent of nonlinearity. Significant deformation has accumulated at the integral deck-abutment-backfill joint. Similar response is observed at the bottom of abutment as shown in Fig. 6(b). Under GM#2 in Fig. 6(c), the top and bottom DTHs of abutment are quite similar and the bridge model has no significant residual response after dynamic analysis; this implies that under GM#2 the structure is linear elastic and remains unyielded. At the top of abutment piles moment rotation curves are plotted in Figs. 7(a) and 7(b) under GM#1 and GM#2, respectively. Under GM#1, the 9span bridge abutment piles yielded and 7span, 5span and 3span bridges' abutment piles remain linear elastic. Under GM#2, 9span bridge's abutment piles show completely linear elastic behaviour. Similar type of nonlinearity is seen at the depth of 3-4m of pier piles in Figs. 7(c) and 7(d) under GM#1 and GM#2, respectively. Under GM#1, 9span, 7span and 5span bridge pier piles undergo severe nonlinearity. Under GM#2, pier piles exhibit linear elastic response, as insignificant energy is distributed over the large frequency range.

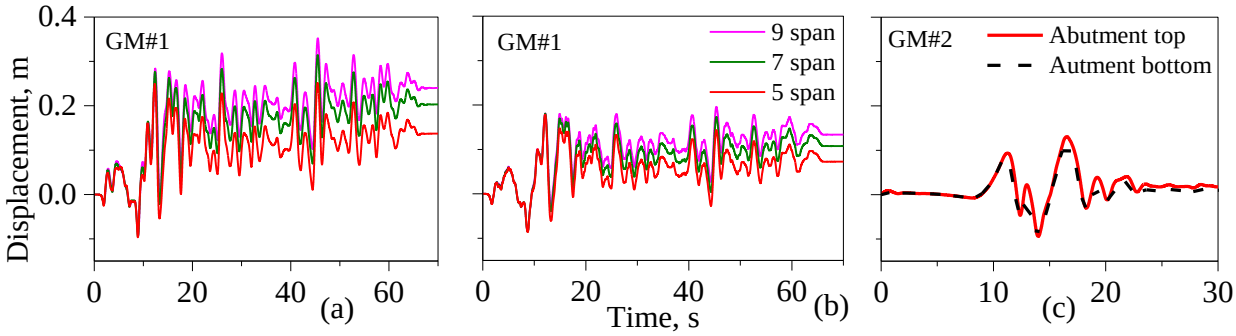

Figure 6. Displacement time history (DTH) at (a) top of abutment and (b) bottom of abutment under GM#1, (c) DTH under GM#2.

It is observed that the 9span bridge underwent inelastic behaviour and significant nonlinearity is observed as compared to the 7span, 5span and 3span bridges after DTHA under GM#1. Hence, an unsuitable length of IB can cause significant differences in dynamic response of the bridge under high intensity of shaking. On the other hand, under low intensity of GMs similar span bridge can easily sustain the dynamic loading and remain linear elastic after the shaking.

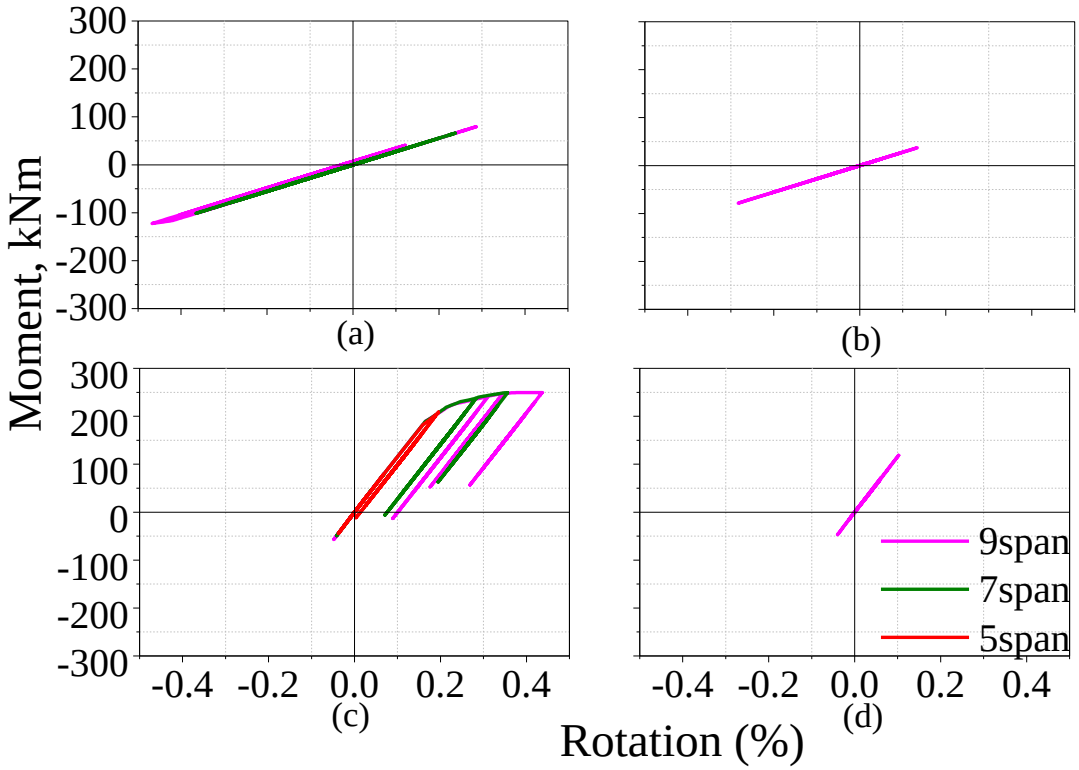

Figure 7. Abutment pile moment-rotation plot under (a) GM#1 and (b) GM#2; Pier pile moment-rotation plot under (a) GM#1 and (b) GM#2.

Response of bridge-foundation in loose sand

Unlike the previous case, pile foundation in loose sand helps the bridge to respond in more flexible manner. In Figs. 8(a) and 8(b), 3rd pier SFTHs are shown under GM#1 and GM#2,

respectively. From the SFTHs, under GM#1, it is visible that 9span bridge deck level has 133kN residual response, but from moment rotation curve at top of pier it shows that it is in elastic range in Fig. 8 (c). 7span bridge under GM#1 and 9span bridge under GM#2 show linear elastic moment-rotation curves at the top of pier in Figs. 8(c) and 8(d), respectively.

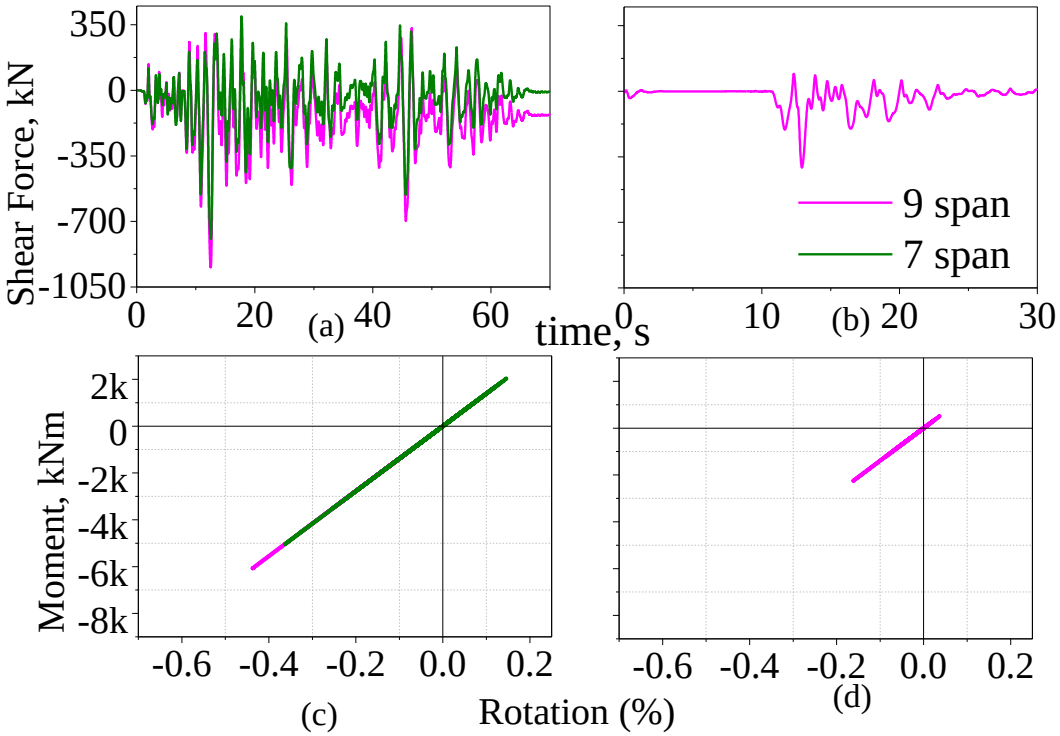

Figure 8. Shear force time history at the top of 3rd pier under (a) GM#1 and (b) GM#2; Moment rotation at the top of 3rd pier under (c) GM#1 and (d) GM#2 in loose sand.

DTHs at the top and bottom of abutments under GM#1 are shown in Figs. 9(a) and 9(b), respectively. For the 9span bridge, the top and bottom of abutment incur residual displacements of 7.6cm and 3.2cm, respectively. Similarly, for the 7span bridge under GM #1 and 9span bridge under GM#2 (in Fig. 9(c)), insignificant residual response is observed after the completion of the dynamic analysis. Thus, the bridge superstructure and substructure are linear elastic in both the cases.

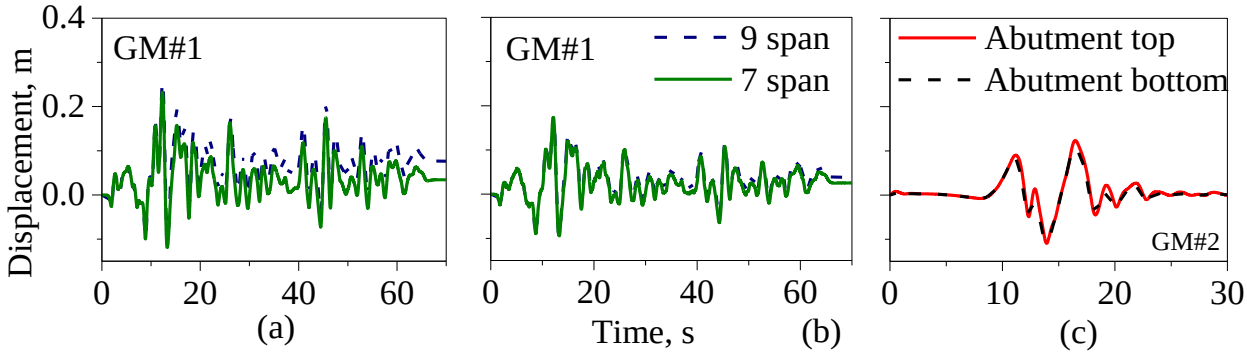

Figure 9. Displacement time history (DTH) at (a) top of abutment and (b) bottom of abutment under GM#1, (c) DTH under GM#2.

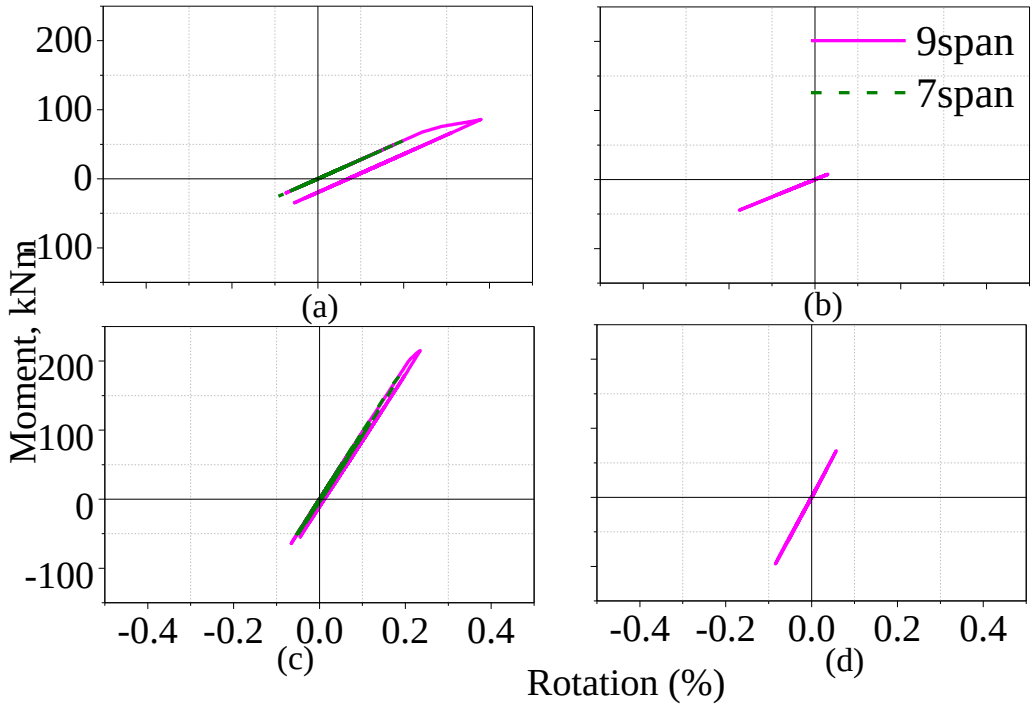

Figure 10. (a) Abutment pile moment-rotation plot under GM#1, (b) abutment pile moment-rotation plot under GM#2, (c) pier pile moment-rotation plot under GM#1 and (d) pier pile moment-rotation plot under GM#2 in loose sand foundation soil.

Under GM#1, the obtained moment-rotation curves for the abutment and the pier piles are shown in Figs. 10(a) and 10(c), respectively. For the 9span bridge, pier and abutments piles have yielded and in shorter span bridges, linear elastic behaviour of the piles is observed. In Figs. 10(b) and 10(d), the moment-rotation curves of the abutment and pier piles are shown under GM#2 and in both the locations, piles show linear elastic response. So, unlike medium stiff clayey soil, only the 9span bridge shows nonlinear response in loose sand and with yielding in the foundation part only. Though, nonlinearity is limited to a depth of 8m of pile length, special attention is needed to design the pile foundation in soft soil for larger jointless bridges.

Comparison of response of bridge in loose sand and medium clay soil

Under GM#1, normalized Fourier transform of SFTHs, at the top of 3rd pier, are plotted in Figs. 11 (a) and (b), under GM#1 and GM#2, respectively. Under GM#1, SFTH in loose sand contains higher forces than medium clayey soil. As, the loose soil induces more deformation in bridge foundation, thus higher deformation is transferred to the bridge structure. So, the structure carries higher SF during THA. But a totally different behavior is observed for the bridge under GM#2 with lower intensity of GM where, the nonlinearities in the structure and the foundation soil are not fully developed. So the foundation in the stiffer soil, i.e., medium stiff clay induces more forces and moments on the overall structure and the superstructure carries more forces as compared to the bridge in loose sand foundation soil under GM#2. In Fig. 11(c), the comparison of average fourier amplitude of seven rock outcrop GMs and output average Frourier transform (blue line) of ATHs monitored at the top of 3rd pier in SAP2000 is shown. The output Fourier amplitude is considerably higher throughout the 0.1-10Hz frequency range. This is because of the

encountered structural and soil nonlinearities of seicmic waves as it get amplified during vertical propagation from bedrock to superstructure level.

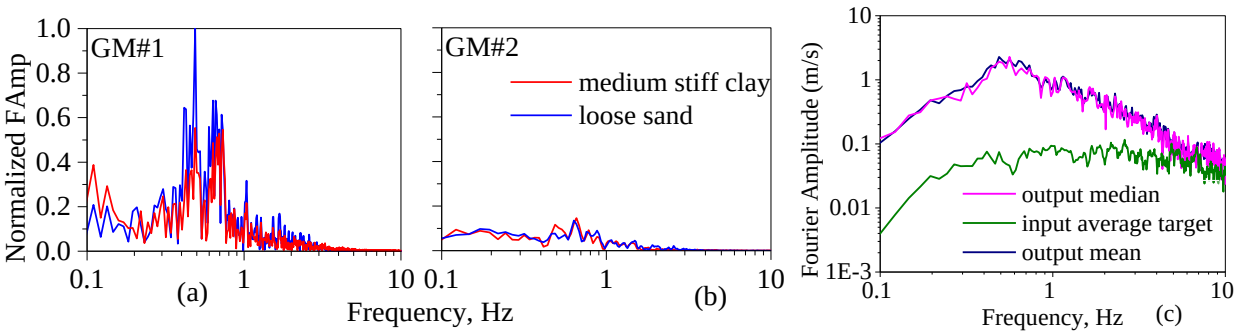

Figure 11. (a) Normalized Fourier transform of SFTH under GM#1, (b) normalized Fourier transform of SFTH under GM#2 at the top of 3rd pier for 9span bridge and (c) comparison of Fourier amplitude at input and output stages of analysis for 9span bridge in medium stiff clayey soil.

Summary

To provide a closure to this study, dynamic analysis is carried out with set of seven GMs. GM#2 and GM#3 (in fig. 4a) contain significantly less amout of seismic energies than the other GMs in the study which is visible from the fourier amplitude plot of GM#2 (in Fig. 4(e)) at different natural frequencies of bridge models. Among the 7 site specific GMs, under GM#2 and GM#3, 9span 7span, 5span and 3span bridges are in linear elastic state in both foundation soil type. Under GM#1 and the rests, 9span bridge has failed either at different locations of piles or both piles and piers, followed by the pile failures in the 7span and 5span bridges. During THA, the 3rd and 6th piers' top locations are the most vulnerable ones in different span bridge models from the superstructure part. The abutment piles and piles from 3rd and 6th intermediate pile groups are more susciptable to form hinges in THA from foundation part. From the present study, it can be concluded that the larger IB attracts more forces and moments than the shorter one as there is no intermediate joint or bearing for energy dissipation which would reduce the shaking at superstructure level. The superstructure members show linear elastic response with the possible hinge formation in the foundation piles during strong earthquake shaking. IBs on loose foundation soil can deform easily and failure of structural members can be limited to the foundation part only. Depending on proper geological investigation and site specific characteristics, IBs should be constructed so that due to larger length, yielding of foundation piles can be prevented. In that case, foundation needs to be designed more carefully with higher endurance capacity and proper retrofitting of foundation should be a scope to make the bridge more sustainable under high intensity GMs.

References

1. Wasserman E, Walker J. Integral abutments for steel bridges. *Tennessee Department of Transportation*, TN, 1996.
2. Itani AM, Pekcan G. Seismic performance of steel plate girder bridges with integral abutments. *U.S. Department of Transportation, Federal Highway Administration.* Report No. FHWA-HIF-11-043, 2011.
3. CSI S. CSi Analysis Reference Manual. I: Berkeley (CA, USA): *Computers and Structures INC,* 2014.

4. Elgamal A, Yan L, Yang Z, Conte JP. Three-dimensional seismic response of Humboldt bridge-foundation-ground system. *Journal of Structural Engineering* 2008; **134**(7):1165–1176.
5. Chang GA, Mander JB. Seismic Energy Based Fatigue Damage Analysis of Bridge Columns: Part I – Evaluation of Seismic Capacity. *NCEER Technical Report* No. NCEER-94-0006, State University of New York, Buffalo, 1994.
6. Prakash S, Sharma HD. *Pile foundations in engineering practice*. John Wiley & Sons, 1990.
7. API RP2A-WSD. *Recommended practice for planning, designing and constructing fixed offshore platforms–working stress design*. 21st Edition, December, 2000.
8. BA 42/96 Amendment No. 1. *Design Manual for Integral Bridges: Design Manual for Road and Bridges.* Volume 1, Section 3, Part 12. The Highway Agency, UK, 2003.
9. Zhang Y, Conte JP, Yang Z, Elgamal A, Bielak J, Acero G. Two dimensional nonlinear earthquake response analysis of a bridge-foundation ground system. *Earthquake Spectra* 2008; **24(**2):343–386.
10. Erhan S, Dicleli M. Parametric study on the effect of structural and geotechnical properties on the seismic performance of integral bridges. *Bulletin of Earthquake Engineering* 2017, **15**(10):1-29.
11. Dhar S, Özcebe AG, Dasgupta K, Dey A, Paolucci R, Petrini L. Nonlinear Dynamic Soil-Structure Interaction Effects on the Seismic Response of a Pile-Supported Integral Bridge Structure. *6th International Conference on Recent Advances in Geotechnical Earthquake Engineering and Soil Dynamics* 2016. Paper No. 141, New Delhi, India.
12. Petersen MD, Frankel AD, Harmsen SC, Mueller CS, Haller KM, Wheeler RL, Wesson RL, Zeng Y, Boyd OS, Perkins DM, Luco N, Field EH, Wills CJ, Rukstales KS. Documentation for the 2008 Update of the United States National Seismic Hazard Maps. U.S. Geological Survey; Open-File Report 2008-1128, 2008.
13. Holzer TL, Padovani AC, Bennett MJ, Noce ET, Tinsley JC, Mapping NEHRP VS30 Site Classes. *Earthquake Spectra* 2005; **21**(2):1-18.
14. Smerzini C, Paolucci R, Galasso C, Iervolino I, *Engineering ground motion selection based on displacement-spectrum compatibility*, Proceedings of the 15th World Conference on Earthquake Engineering 2012; Paper no**. 2354**, Lisbon, Portugal.
15. Smerzini C, Galasso C, Iervolino I, Paolucci R, Ground motion record selection based on broadband spectral compatibility, *Earthquake Spectra* 2014; **30**(4): 1427-1448.
16. AASHTO LRFD, *Bridge Design Specifications (6th ed.)*. Washington, DC: American Association of State Highway and Transportation Officials, 2012.